Published in final edited form as:
Cancer Cell. 2012 December 11; 22(6): 737–750. doi:10.1016/j.ccr.2012.10.025.

Identification of Sox9-dependent acinar-to-ductal reprogramming as the principal mechanism for initiation of pancreatic ductal adenocarcinoma

Janel L. Kopp[1,*], **Guido von Figura**[2,*], **Erin Mayes**[1], **Fen-Fen Liu**[1], **Claire L. Dubois**[1], **John P. Morris IV**[2], **Fong Cheng Pan**[3], **Haruhiko Akiyama**[4], **Christopher V. E. Wright**[3], **Kristin Jensen**[5], **Matthias Hebrok**[2,†], and **Maike Sander**[1,†]

[1]Departments of Pediatrics and Cellular & Molecular Medicine, University of California-San Diego, La Jolla, CA 92093-0695

[2]Diabetes Center, Department of Medicine, University of California-San Francisco, San Francisco, CA 94143

[3]Department of Cell and Developmental Biology, Vanderbilt University, Nashville, TN 37232-8240

[4]Department of Orthopedics, Kyoto University, 54 Kawahara-cho, Shogoin, Sakyo, Kyoto 606-8507, Japan

[5]Department of Pathology, Veterans Affairs Palo Alto Health Care System and Stanford University Hospital, Stanford, CA 94305

Summary

Tumors are largely classified by histological appearance, yet morphological features do not necessarily predict cellular origin. To determine the origin of pancreatic ductal adenocarcinoma (PDA), we labeled and traced pancreatic cell populations after induction of a PDA-initiating Kras mutation. Our studies reveal that ductal and stem-like centroacinar cells are surprisingly refractory to oncogenic transformation, whereas acinar cells readily form PDA precursor lesions with ductal features. We show that formation of acinar-derived premalignant lesions depends on ectopic induction of the ductal gene *Sox9*. Moreover, when concomitantly expressed with oncogenic Kras, *Sox9* accelerates formation of premalignant lesions. These results provide insight into the cellular origin of PDA and suggest that its precursors arise via induction of a duct-like state in acinar cells.

Introduction

Defining tumor-initiating events is critically important for developing early cancer detection methods and effective treatments. In the past, the cell type responsible for tumor initiation has often been inferred based on the histological appearance of the tumor. However,

[†]Corresponding authors: masander@ucsd.edu, Telephone: (858) 246-0843, Fax: (858) 246-1579. hebrok@diabetes.ucsf.edu, Telephone: (415) 514-0820, Fax: (415) 564-5813.
[*]These authors contributed equally to this work

Supplemental Information
Supplemental Information includes Supplemental Experimental Procedures, five figures and one table.

The authors have no conflicts of interest.

morphological features do not necessarily predict a lineage relationship (Goldstein et al., 2010), which can only be determined by lineage tracing studies.

Invasive PDA is believed to arise from a spectrum of preneoplastic mucinous lesions with ductal morphology, namely pancreatic intraepithelial neoplasias (PanINs), the most common precursor lesions observed in humans, as well as mucinous cystic neoplasias (MCNs) and intraductal papillary mucinous neoplasias (IPMNs) (Hezel et al., 2006). During disease progression, accumulation of genetic mutations in these lesions leads to an increasing degree of atypia and ultimately PDA (Feldmann et al., 2007). The earliest detectable mutations found in preneoplastic lesions are activating mutations of the *Kras* gene (Kanda et al., 2012). The significance of *Kras* mutations for disease initiation has been demonstrated in mice, where expression of the constitutively active $Kras^{G12D}$ allele induces PanINs and after a significant latency period also PDA (Hingorani et al., 2003). In $Kras^{G12D}$-expressing mice, PanIN formation coincides with, or is preceded by, acinar-to-ductal metaplasia (ADM), characterized by replacement of acinar cells with cells expressing ductal markers, such as *CK19* and the ductal fate determinant *Sox9* (Morris et al., 2010; Zhu et al., 2007). ADM is also observed in pancreatitis, which is a significant risk factor for PDA in humans (Lowenfels et al., 1993) and accelerates $Kras^{G12D}$-mediated PanIN and PDA formation in mice (Carriere et al., 2009; Guerra et al., 2007; Morris et al., 2010). These findings imply that oncogenic *Kras* mutations induce ADM, PanINs and ultimately PDA. However, it is still unclear whether ADM and PanINs primarily arise by expansion of ductal cells and secondary replacement of acinar cells or by direct reprogramming of acinar cells into cells with ductal morphology.

Because previous studies have modeled PDA initiation mostly by expressing oncogenic Kras in all cell types of the pancreas (Aguirre et al., 2003; Hingorani et al., 2003; Hingorani et al., 2005), little is known about its cell of origin. In mice deficient for the tumor suppressor *Pten*, the formation of invasive pancreatic cancer is associated with increased proliferation of centroacinar cells (CACs) (Stanger et al., 2005), which reside at the tips of the ductal tree. CACs express some markers of embryonic pancreatic progenitors and exhibit features of tissue stem cells *in vitro* (Miyamoto et al., 2003; Rovira et al., 2010). Since numerous tumors have been shown to originate from tissue stem cells (Visvader, 2011), it has been proposed that CACs are the cell of origin for PanINs and PDA (Miyamoto et al., 2003; Stanger et al., 2005). However, this contention has not been directly tested, largely because genetic tools to target ductal and CACs have only recently been generated (Kopp et al., 2011; Solar et al., 2009). Genetic studies, using *CK19* promoter-based alleles to activate oncogenic *Kras* in ductal cells, suggest that PanINs rarely arise from ducts (Brembeck et al., 2003; Ray et al., 2011). Yet, the rather exclusive targeting of larger ducts in these studies precluded assessing susceptibility of CACs to $Kras^{G12D}$-mediated PanIN induction.

Previous studies have shown that oncogenic *Kras* can convert acinar cells into duct-like cells and PanINs (Carriere et al., 2007; De La O et al., 2008; Guerra et al., 2007; Habbe et al., 2008; Morris et al., 2010). While these studies suggest acinar-to-ductal reprogramming (ADR) as a possible mechanism for initiating PanINs, it is unclear whether PanINs are more readily induced after direct oncogenic transformation of ductal or CACs. Moreover, it is unknown whether inducers of ductal cell identity, such as *Sox9* (Delous et al., 2012; Shih et al., 2012), play a role in the induction of PanINs from acinar cells.

In this study, we directly compared the propensity of ductal/CACs and acinar cells to form PanINs and investigated the molecular mechanisms that underlie PanIN formation.

Results

Sox9 is expressed in human premalignant and malignant pancreatic lesions

Under normal conditions, the transcription factor Sox9 is expressed in ductal and CACs, but not acinar cells (Seymour et al., 2007). In addition, Sox9 is induced during ADM and expressed in PanINs and PDA (Morris et al., 2010; Prevot et al., 2012). To comprehensively examine SOX9 expression in the human pancreas, we employed a tissue microarray for immunohistochemical analysis of SOX9 expression in different pancreatic lesions (Figure 1A–H). SOX9 was expressed in chronic pancreatitis, as well as premalignant and malignant lesions, including MCNs, IPMNs, PanINs, and PDA. Low-grade PanINs were uniformly $SOX9^+$, whereas higher-grade PanIN2/3 lesions and PDA displayed heterogeneous SOX9 expression (Figure 1l; 72% of PanIN2/3 and 69% of PDA were $SOX9^+$). These findings suggest that a $SOX9^+$ state is associated with PDA initiation.

Kras^{G12D}-induced PanINs predominantly arise from acinar but not ductal/centroacinar cells

To determine whether PanINs arise from Sox9-expressing ductal/CACs or from acinar-derived duct-like cells ectopically expressing Sox9, we directly compared the propensity of ductal/CACs and acinar cells to form PanINs in response to oncogenic Kras. To inducibly recombine the *LSL-Kras^{G12D}* allele (hereafter referred to as the *Kras^{G12D}* allele) in ductal/CAC or acinar cells, we used *Sox9CreER* or *Ptf1a^{CreER}* mice, respectively. The Cre-dependent *R26R^{YFP}* reporter allele was included to assess recombination efficiency and map the fate of Kras-active cells. Four days after induction of recombination by tamoxifen at postnatal day 10 (p10), we analyzed pancreatic labeling specificity and efficiency by quantifying the percentage of ductal and acinar cells expressing YFP (Figure 2A; Figure S1A). As previously reported (Kopp et al., 2011), the *Sox9CreER* transgene labeled cells throughout the entire ductal tree, including CACs (Figure S1B, C; data not shown). On average, we labeled 12% of all $Sox9^+$ cells with the *Sox9CreER* transgene and 10% of $Cpa1^+$ acinar cells with the *Ptf1a^{CreER}* allele (Figure 2B; Figure S1D, E). Quantification of non-lineage-specific recombination events revealed *R26R^{YFP}* recombination in 0.02% of acinar cells by *Sox9CreER* and 0.23% of $Sox9^+$ cells by *Ptf1a^{CreER}* (Figure 2B). A similar pattern of YFP expression was observed after 8 months or longer (Figure 2I, K), confirming that acinar and ductal cells do not spontaneously convert into other pancreatic cell types (Desai et al., 2007; Kopp et al., 2011; Solar et al., 2009; Strobel et al., 2007). Overall, this analysis shows that the *Sox9CreER* transgene and *Ptf1a^{CreER}* allele specifically target the ductal/CAC and acinar cell compartments, respectively. Moreover, the *Kras^{G12D}* allele was effectively recombined by both *Ptf1a^{CreER}* and *Sox9CreER* (Figure S1F).

To assess the frequency of PanINs arising from acinar or ductal/CACs after Kras activation, we examined pancreata from *Ptf1a^{CreER};Kras^{G12D};R26R^{YFP}* and *Sox9CreER;Kras^{G12D};R26R^{YFP}* mice 8 to 17 months after *Kras^{G12D}* induction (Figure 2A). Corroborating previous studies, showing that Kras activation in acinar cells can induce PanINs (Carriere et al., 2007; De La O et al., 2008; Gidekel Friedlander et al., 2009; Guerra et al., 2007; Habbe et al., 2008), all *Ptf1a^{CreER};Kras^{G12D};R26R^{YFP}* mice displayed abundant lesions with histological and molecular characteristics of PanINs, including high acidic mucin content, indicated by Alcian blue staining, and expression of Muc5AC and Claudin18 (Figure 2C–F; Figure S1G, H; Table 1). Expression of YFP further confirmed that the PanINs originated from acinar cells (Figure 2J).

In contrast to *Ptf1a^{CreER};Kras^{G12D};R26R^{YFP}* mice, pancreatic histology was largely normal in *Sox9CreER;Kras^{G12D};R26R^{YFP}* mice and PanINs were rarely observed (Figure 2C, G). Out of 14 mice, no PanINs were detected in 6 mice and the remaining mice had no more

than 10 PanINs per mouse (Table 1; Table S1). As seen in PanINs originating from acinar cells (Figure 2F; Figure S1G, H), the duct-derived lesions were Alcian blue^{+} (Figure 2H, inset), expressed Muc5AC and Claudin18 (Figure S1I, J) and the lineage marker YFP (Figure 2L). However, unlike acinar-derived PanINs, the duct-derived lesions were not randomly distributed throughout the pancreas, but were more often associated with large ducts (Figure S1J, arrow).

To thoroughly compare the extent of PanIN formation from acinar and ductal/CACs, we quantified the Alcian blue^{+} area in *Ptf1a^{CreER};Kras^{G12D};R26R^{YFP}* and *Sox9CreER;Kras^{G12D};R26R^{YFP}* mice on sections spaced every 140 μm throughout the entire pancreas (Figure 2M). Notably, Alcian blue staining can be present in duct-like lesions devoid of neoplastic features and conversely, can be absent from high-grade PanIN lesions (Cornish and Hruban, 2011; Strobel et al., 2007). Since the majority of Alcian blue^{+} lesions in *Ptf1a^{CreER};Kras^{G12D};R26R^{YFP}* and *Sox9CreER;Kras^{G12D};R26R^{YFP}* mice exhibited neoplastic characteristics of PanINs and Alcian blue^{-} PanINs were rarely observed (Figure S1K and data not shown), Alcian blue staining appeared to be an accurate measure PanIN frequency in these models. In *Ptf1a^{CreER};Kras^{G12D};R26R^{YFP}* mice, on average 6.7±1.5% of the pancreas was Alcian blue^{+}. In contrast, only 0.013±0.004% of the pancreas exhibited Alcian blue staining in *Sox9CreER;Kras^{G12D};R26R^{YFP}* mice (Figure 2M). While this result suggests a striking difference in the propensity of acinar and ductal/CACs to give rise to PanINs, this quantification likely overestimates the difference, because acinar cells are more abundant than ductal cells and therefore a larger overall number of cells will express *Kras^{G12D}* in *Ptf1a^{CreER};Kras^{G12D};R26R^{YFP}* than in *Sox9CreER;Kras^{G12D};R26R^{YFP}* mice. To account for this difference, we quantified the total number of recombined YFP^{+} cells in *Sox9CreER;R26R^{YFP}* and *Ptf1a^{CreER};R26R^{YFP}* mice 4 days after tamoxifen injection. After accounting for the 4.6-fold difference (Figure S1L), *Ptf1a^{CreER}*-induced Kras activation still resulted in a 112-fold higher frequency of PanINs than *Sox9CreER*-mediated Kras activation (Figure 2M). These data show that acinar cells have a much greater propensity than ductal/CACs to form PanINs in response to oncogenic Kras (Figure 2N).

Acute pancreatitis promotes *Kras^{G12D}*-mediated PanIN formation from acinar, but not ductal cells

Previous studies have shown that caerulein-induced acute or chronic pancreatitis accelerates *Kras^{G12D}*-mediated PanIN and PDA formation (Carriere et al., 2009; Gidekel Friedlander et al., 2009; Guerra et al., 2007; Morris et al., 2010). In the absence of oncogenic *Kras*, acute pancreatitis induces transient ADM followed by reversion to normal acinar cell morphology (Jensen et al., 2005; Morris et al., 2010). By contrast, acute pancreatitis in the presence of oncogenic Kras leads to persistent ADR and accelerated PanIN formation (De La O and Murtaugh, 2009; Morris et al., 2010). To compare how pancreatitis affects PanIN formation after ductal or acinar cell-specific Kras activation, we induced caerulein-mediated acute pancreatitis in 6-week-old *Ptf1a^{CreER};Kras^{G12D};R26R^{YFP}*, *Sox9CreER;Kras^{G12D};R26R^{YFP}* and control mice and analyzed pancreatic tissue 2 or 21 days later (Figure 3A; Figure S2A). As reported (Morris et al., 2010), 2 days post-caerulein treatment control mice exhibited widespread ADM with characteristic degranulation of acinar cells and appearance of cuboidal to columnar duct-like structures with enlarged lumens (Figure 3B, C), which were replaced by normal acini within 21 days (Figure 3D, E). In *Ptf1a^{CreER};Kras^{G12D};R26R^{YFP}* mice treated with saline, pancreas morphology was largely normal, although small areas of ADM and occasional PanINs were already evident by 9 weeks of age (Figure 3F, inset). Similar to control mice, caerulein induced widespread ADM within 2 days (Figure 3F, G). However, these changes were not transient and duct-like structures were replaced by PanINs after 21 days (Figure 3H, I). These observations are consistent with previous findings (Morris et al., 2010) and confirm that acute pancreatitis promotes PanIN formation from

Kras^{G12D}-expressing acinar cells. In contrast to *Ptf1a*^{CreER};*Kras*^{G12D};*R26R*^{YFP} mice, virtually no PanINs were observed 21 days after caerulein treatment of *Sox9CreER;Kras*^{G12D};*R26R*^{YFP} mice (Figure 3J–M; Table 1; Table S1) and pancreas morphology was similar to control mice not expressing oncogenic Kras (Figure 3D, E). These results suggest that *Kras*^{G12D}-expressing ductal cells have a low propensity to form PanINs even when exposed to pro-neoplastic insults, such as acute pancreatitis.

To directly compare how pancreatitis affects PanIN formation from *Kras*^{G12D}-expressing acinar and ductal/CACs, we quantified the Alcian blue^{+} area, which was predominately composed of PanIN lesions (data not shown and Figure S2B), in *Sox9CreER;Kras*^{G12D};*R26R*^{YFP} and *Ptf1a*^{CreER};*Kras*^{G12D};*R26R*^{YFP} mice 21 days after caerulein treatment (Figure 3N). In mice expressing *Kras*^{G12D} in acinar cells, caerulein induced a significant 20.9-fold increase in Alcian blue^{+} area. By contrast, no significant increase was observed in *Sox9CreER;Kras*^{G12D};*R26R*^{YFP} mice. Examination of individual mice revealed an increase in the overall number of mice exhibiting Alcian blue^{+} PanINs in caerulein-treated compared to saline-treated *Sox9CreER;Kras*^{G12D};*R26R*^{YFP} mice (Table 1; 3/5 mice had PanINs after caerulein treatment *vs.* 1/9 mice after saline treatment). However, in mice with PanINs a total of only 1–2 PanINs were found per pancreas (Table S1). Overall, the Alcian blue^{+} area in caerulein-treated *Sox9CreER;Kras*^{G12D};*R26R*^{YFP} mice was similar to controls not expressing the *Kras* oncogene (Figure 3N). Together, these data demonstrate that acute pancreatitis potentiates PanIN formation from *Kras*^{G12D}-expressing acinar cells, but not from *Kras*^{G12D}-expressing ductal/CACs (Figure 3O).

Sox9 is necessary for *Kras*^{G12D}-mediated PanIN induction

Given that ADM and early PanINs are Sox9^{+} (Figure 1; Morris et al., 2010; Prevot et al., 2012), but Sox9^{+} ductal cells are not the predominant source of PanINs, we examined whether Sox9 is induced in *Kras*^{G12D}-expressing acinar cells prior to ADM. In control mice, Sox9 expression was restricted to ductal and CACs (Figure 4A, C, arrowheads). In *Ptf1a*^{Cre};*Kras*^{G12D} mice, Sox9 was additionally detected in a subset of cells with acinar morphology, expressing the acinar marker Cpa1, but not the ductal marker CK19 (Figure 4B, D, arrows). These data indicate that Sox9 expression is initiated before Kras-active acinar cells progress to a duct-like state and become PanINs.

Since *Sox9* is important for ductal cell development and regulates critical ductal genes (Shih et al., 2012), we examined whether *Sox9* plays a role in the transformation of acinar cells into ductal structures and premalignant lesions. To test if *Sox9* is required for PanIN formation, we concomitantly induced *Kras*^{G12D} expression and deleted *Sox9* in acinar cells in 3-week-old *Ptf1a*^{CreER};*Kras*^{G12D};*Sox9*$^{f/f}$;*R26R*^{YFP} mice (Figure 4E; Figure S3A). Consistent with the lack of Sox9 expression in normal acinar cells, acinar cell-specific *Sox9* deletion did not affect gross acinar cell morphology or the pattern of pancreatic Sox9 expression (Figure 4F, I, L, O). Next, we analyzed 8–12-month-old *Ptf1a*^{CreER};*Kras*^{G12D};*Sox9*$^{+/+}$;*R26R*^{YFP} and *Ptf1a*^{CreER};*Kras*^{G12D};*Sox9*$^{f/f}$;*R26R*^{YFP} mice for the presence of PanINs. Confirming our previous findings (Figure 2E, F), pancreata from *Ptf1a*^{CreER};*Kras*^{G12D};*Sox9*$^{+/+}$;*R26R*^{YFP} mice contained widespread Alcian blue^{+} PanIN lesions, expressing the YFP lineage label and Sox9 (Figure 4G, J, M, P). In striking contrast, pancreas morphology was virtually normal in *Sox9*-deleted mice and very few PanINs were observed (Figure 4F, I, H, K). Quantification of Alcian blue staining revealed a 153-fold reduction in the Alcian blue^{+} area in *Sox9*-deleted *Ptf1a*^{CreER};*Kras*^{G12D} mice compared to mice with two functional *Sox9* alleles (Figure 4AD). Notably, PanINs that still formed in *Ptf1a*^{CreER};*Kras*^{G12D};*Sox9*$^{f/f}$;*R26R*^{YFP} mice were YFP^{+} and Sox9^{+} (Figure 4N, Q), indicating that these PanINs arose from acinar cells that recombined the *R26R*^{YFP} and *Kras*^{G12D} alleles, but not the *Sox9*^{flox} allele. Together, these findings demonstrate that PanIN formation from Kras-active acinar cells requires Sox9 activity (Figure S3R).

Sox9 promotes *Kras^{G12D}*-mediated induction of PanINs

Given the critical role of *Sox9* in PanIN formation and its early induction in Kras-active acinar cells, we next examined whether forced expression of *Sox9* potentiates *Kras^{G12D}*-mediated PanIN formation. To test this idea, we crossed the well-characterized *Ptf1a^{Cre};Kras^{G12D}* model of PanIN formation (Hingorani et al., 2003) with mice harboring a Cre-inducible *Sox9* transgene (*CAG-Sox9,* hereafter referred to as *Sox9^{OE}*). In *Sox9^{OE}* mice, *RFP* is ubiquitously expressed in all cells unless Cre-mediated excision removes the *RFP* sequence and induces heritable expression of a bicistronic transcript encoding *GFP* and HA-tagged *Sox9* (Figure S3B). Consistent with the propensity of *Ptf1a^{Cre}* to mostly target acinar cells (Heiser et al., 2008), *Ptf1a^{Cre};Sox9^{OE}* mice expressed the HA-tag and Sox9 predominantly in acinar cells, whereas ducts and endocrine clusters remained largely unrecombined and retained RFP (Figure S3E–G, J–L). In 3-week-old *Ptf1a^{Cre};Sox9^{OE}* mice, pancreatic weight, overall tissue morpholo gy and blood glucose levels were similar to control mice (Figure S3C, D, H, I, M, N), suggesting that *Ptf1a^{Cre}*-mediated *Sox9* misexpression has no overt effect on pancreatic development.

Similar to *Ptf1a^{Cre};Sox9^{OE}* mice, *Ptf1a^{Cre};Kras^{G12D};Sox9^{OE}* mice also developed normally until 3 weeks of age (data not shown), but thereafter began to exhibit signs of exocrine insufficiency and changes in gross pancreatic morphology not seen in *Ptf1a^{Cre};Kras^{G12D}* or *Ptf1a^{Cre};Sox9^{OE}* mice (Figure S3O–Q; data not shown). Synergy between *Sox9* and *Kras^{G12D}* was also observed at a microscopic level, as evidenced by replacement of normal pancreas parenchyma by large areas of Sox9^{+} ADM and Alcian blue^{+} PanINs in *Ptf1a^{Cre};Kras^{G12D};Sox9^{OE}* mice (Figure 4T, W, AC); a phenotype not seen in age-matched *Ptf1a^{Cre};Kras^{G12D}* or control mice (Figure 4R, S, U, V, X, Y, AA, AB). The pancreatic area occupied specifically by Alcian blue^{+} PanIN lesions was 17-fold greater in *Ptf1a^{Cre};Kras^{G12D};Sox9^{OE}* than in *Ptf1a^{Cre};Kras^{G12D}* mice (Figure 4AE). Detection of the HA-tag in both ADM and PanIN lesions further demonstrated that they arose from cells expressing the *Sox9^{OE}* transgene (Figure 4Z). Because *Ptf1a^{Cre}* predominantly targets acinar cells (Figure S3K, L), these findings suggest that concomitant misexpression of *Sox9* and *Kras^{G12D}* rapidly induces transformation of acinar cells into duct-like cells and subsequent PanIN formation. Consistent with this notion, very few cells retained Cpa1 in *Ptf1a^{Cre};Kras^{G12D};Sox9^{OE}* mice and CK19^{+} ductal structures were predominant (Figure 4AF). Within these structures, few CK19^{+} cells coexpressed Cpa1 (Figure 4AF, arrows), indicating that most cells had already transitioned from a CK19^{+}Cpa1^{+} into a CK19^{+}Cpa1^{-} state characteristic of ADR (De La O et al., 2008; Morris et al., 2010). Together, these results suggest that *Sox9* accelerates *Kras^{G12D}*-mediated PanIN formation by suppressing a mature acinar cell program and/or promoting a duct-like state (Figure S3R).

Sox9 induces ductal genes in acinar cells

To determine whether forced expression of *Sox9* in acinar cells induces a duct-like state in the absence of oncogenic Kras, we examined *Ptf1a^{Cre};Sox9^{OE}* mice for coexpression of CK19 with Cpa1. In *Ptf1a^{Cre};Sox9^{OE}* mice at 3 weeks of age or older, Cpa1 colocalized with CK19, whereas the two domains remained separate in control mice (Figure 5A–F). QRT-PCR confirmed the increase in *CK19* and also revealed a decrease in acinar cell-specific genes (Figure 5I). While these molecular changes are indicative of acinar cell de-differentiation, the CK19^{+}Cpa1^{+} cells largely retained acinar morphology and did not form duct-like structures (Figure 5E–H, J, K). This suggests that *Sox9* expression in acinar cells destabilizes the acinar cell state and promotes expression of ductal genes, but is not sufficient to induce complete ductal reprogramming.

Sox9 promotes acinar-to-ductal reprogramming and induces mucinous metaplasia after pancreatic injury

Although Kras activation induces ADM and PanINs, it does so with considerable latency, which is significantly shortened in the presence of pancreatitis (De La O and Murtaugh, 2009; Guerra et al., 2007; Morris et al., 2010). To test whether Sox9, like oncogenic Kras, requires inflammatory cues to initiate widespread ADM, we induced acute pancreatitis in *Ptf1a*^{Cre};*Sox9*^{OE} mice. Injection with caerulein on consecutive days (Figure 6A) resulted in loss of acinar morphology and induction of Sox9 and CK19 in a subset of Cpa1^{+} cells 2 days after treatment (Figure 6C, I, O). In control mice, normal pancreatic morphology was restored after 7 days and CK19 and Sox9 expression was again restricted to ductal cells (Figure 6B, D, H, J, N, P). Two days after caerulein administration, *Ptf1a*^{Cre};*Sox9*^{OE} mice displayed more severe ductal metaplasia than control mice (Figure 6C, F) with numerous CK19^{+}Cpa1^{-} and Sox9^{+} cell clusters (Figure 6L, R). After 7 days, acinar morphology was not restored and CK19^{+}Cpa1^{-} ductal structures characteristic of ADR persisted (Figure 6E–G, K–M, Q–S). These findings show that *Sox9* misexpression is sufficient to promote reprogramming of acinar cells into a persistent duct-like state after pancreatic injury. Interestingly, a subset of the persistent ductal structures that arose from cells expressing the *Sox9*^{OE} transgene were Sox9^{+}Alcian blue^{+} (Figure S4A–G; Figure 6S). These lesions displayed morphological similarity to mucinous lesions observed in a chronic pancreatitis model (Strobel et al., 2007) with little cellular atypia and low amounts of acidic mucins compared to Kras^{G12D}-induced PanINs. Since acute pancreatitis alone is not sufficient to induce mucinous duct-like lesions, our data suggest that persistent expression of Sox9 in acinar cells in the context of tissue injury can initiate a cell state with some characteristics of mucinous PDA precursor lesions (Figure 6T).

Sox9 is not absolutely required for injury-induced acinar-to-ductal metaplasia but necessary for further progression into PanINs

Deletion of *Sox9* in the presence of oncogenic *Kras* completely blocked *Kras*^{G12D}-mediated changes in pancreas morphology, including the development of ADM and PanINs (Figure 4E–Q). However, it remains unclear whether pancreatic injury can still induce ADM and premalignant lesions in the absence of *Sox9*. To address this question, we deleted *Sox9* in acinar cells and examined pancreata for ADM after caerulein treatment (Figure S4H). As expected, control mice exhibited transient ADM characterized by ectopic Sox9 and CK19 expression in acinar cells 2 days after caerulein treatment (Figure S4J, P, V, arrows). Similar lesions devoid of Sox9 were found in caerulein-treated *Ptf1a*^{CreER};*Sox9*$^{f/f}$ mice (Figure S4M, S, Y, arrows), suggesting that Sox9 activity is not absolutely required to initiate ADM. In both control and *Sox9*-deleted mice, areas of ADM were replaced by normal acinar tissue after 7 days (Figure S4I, K, L, N, O, Q, R, T, U, W, X, Z). These data suggest that pancreatic injury can induce ADM-initiating cues independent of *Sox9*.

The finding that pancreatitis causes ADM even in the absence of *Sox9* raises the question of whether *Sox9*-deleted acinar cells can undergo ADR and form PanINs if expression of oncogenic Kras is combined with pancreatic injury. To first examine whether *Sox9* is necessary for *Kras*^{G12D}-mediated ADR, we deleted *Sox9* and activated *Kras*^{G12D} expression in *Ptf1a*^{CreER};*Kras*^{G12D};*Sox9*$^{f/f}$ mice at 3 weeks of age and induced acute pancreatitis 3 weeks later (Figure 7A; Figure S5A). Because Kras had only been active for 6 weeks, PanINs were still rare in *Ptf1a*^{CreER};*Kras*^{G12D};*Sox9*$^{+/+}$ mice in the absence of caerulein (Figure 7G). Caerulein induced widespread formation of Sox9^{+} ADM in *Ptf1a*^{CreER};*Sox9*$^{+/+}$ and *Ptf1a*^{CreER};*Kras*^{G12D};*Sox9*$^{+/+}$ mice within 2 days after treatment (Figure 7B, C, G, H; Figure S5B, C, E, F). Notably, in *Sox9*-deleted *Ptf1a*^{CreER};*Kras*^{G12D};*Sox9*$^{f/f}$ pancreata, Sox9^{-} duct-like structures were still present (Figure 7L, M; Figure S5H, I, arrows), confirming our previous observation that *Sox9* is not absolutely required for injury-induced

ADM. As expected, ADM was transient in the absence of *Kras*^{G12D} and the ductal structures were replaced by Cpa1^{+} acini after 21 days (Figure 7B, D, E; Figure S5B, D). In contrast, Kras-active *Ptf1a*^{CreER}*;Kras*^{G12D}*;Sox9*$^{+/+}$ mice displayed persistent Sox9^{+} ADM (Figure 7I; Figure S5G, arrows), CK19^{+}Cpa1^{-} duct-like structures (Figure 7J, arrow), as well as numerous Sox9^{+} lesions with morphological characteristics of PanINs (Figure 7J, K; Figure S5G, arrowheads). Significantly, *Sox9* deletion in the presence of oncogenic Kras abrogated caerulein-induced PanIN formation, while some Sox9^{-}CK19^{+}Cpa1^{-} duct-like lesions persisted (Figure 7N, O; Figure S5J, arrows). Consistent with these findings, numerous Alcian blue^{+} cells were detected in *Ptf1a*^{CreER}*;Kras*^{G12D}*;Sox9*$^{+/+}$ mice, but virtually none in *Ptf1a*^{CreER}*;Kras*^{G12D}*;Sox9*$^{f/f}$ mice (Figure 7F, K, P, Q). Remaining Alcian blue^{+} lesions in *Ptf1a*^{CreER}*;Kras*^{G12D}*;Sox9*$^{f/f}$ mice were Sox9^{+} (Fig. S5K–M) and therefore escaped recombination. Together, these findings show that pancreatic injury can, at least partially, overcome the block in ADM caused by *Sox9* inactivation in Kras-active acinar cells, but cannot induce PanINs in the absence of *Sox9* (Figure 7R). Thus, *Sox9* is critically required for reprogramming of acini into PanINs.

Discussion

The cellular origin of PanINs

Our study demonstrates that acinar cells exhibit a much higher propensity to form PanINs after oncogenic mutation of *Kras* than ductal or CACs. This finding was surprising, because PDA has been suggested to originate from CACs due to shared molecular features between PanINs and CACs. Notably, although exceedingly low in frequency, PanINs were observed after *Sox9CreER*-mediated *Kras*^{G12D} activation. Since the *Sox9CreER* transgene also induces recombination in a small number of acinar cells, one possibility is that these rare PanINs originated from acinar cells that recombined the *Kras*^{G12D} allele. However, we observed that the PanINs were predominantly associated with large pancreatic ducts, which argues against an acinar origin. A similar association of PanINs with large ducts has been described in *CK19*^{CreER}*;Kras*^{G12D} mice, a model in which recombination is mainly induced in large ducts and not in small ducts or CACs (Ray et al., 2011). Together, these observations suggest that large pancreatic ducts, but not CACs, can give rise to PanINs, albeit at an extremely low frequency.

The location of PanINs close to large ducts points to a possible involvement of pancreatic duct glands in PanIN formation. Pancreatic duct glands are small blind-ended pouches within the larger pancreatic ducts that express embryonic progenitor markers, proliferate in response to pancreatitis, and display some metaplastic features similar to PanINs even in the absence of oncogenic mutations (Strobel et al., 2010). These features may render pancreatic duct glands susceptible to transformation by oncogenic Kras. The scarcity of pancreatic duct glands within the organ could explain why despite targeting of duct glands by the *Sox9CreER* transgene (Kopp et al., 2011), PanIN frequency was extremely low in *Sox9CreER;Kras*^{G12D} mice. Of note, because recombination was only induced in 12% of all Sox9^{+} cells by our tamoxifen regimen, the duct glands may not have been targeted in every mouse, which is consistent with the absence of PanINs in a subset of *Sox9CreER;Kras*^{G12D} mice. At present, very little is known about the biological role of pancreatic duct glands, but their possible involvement in PDA initiation warrants further investigation.

Our finding that normal ductal and CACs do not readily form PanINs in response to oncogenic Kras raises the question of whether the ductal/CAC compartment is generally refractory to oncogenic transformation. In addition to activating mutations in *Kras*, loss-of-function mutations in the tumor suppressors *p53*, *p16* or *Pten* have also been found in PDA (Feldmann et al., 2007; Kanda et al., 2012; Ying et al., 2011). Notably, *Pten* loss results in rapid formation of invasive carcinoma, which is preceded by significant expansion of CACs

(Stanger et al., 2005). This suggests that CACs, ductal cells and acinar cells may have the potential to initiate invasive carcinoma, but that each cellular context may require a different repertoire of genetic alterations for tumor initiation. Cell-specific induction of different oncogenic mutations in mice may define morphologically and molecularly distinct tumors, which may help identify human PDA subtypes that respond differently to therapeutic intervention.

Duct-associated genes orchestrate the emergence of premalignant lesions from acinar cells

Our cell tracing studies show that the predominant mechanism by which $Kras^{G12D}$ induces PanINs is to initiate a gene expression program similar to pancreatic ducts in acinar cells. We further show that the transcription factor Sox9 promotes, and is required for, PanIN formation from the acinar cell compartment. Recent studies have revealed a role for *Sox9* in maintaining ductal cell morphology and regulating duct-specific genes (Delous et al., 2012; Manfroid et al., 2012; Shih et al., 2012), suggesting that Sox9 might have a similar function during acinar cell conversion into PanINs. Consistent with this notion, we found that Sox9 induces *CK19* expression and promotes ADR in the presence of $Kras^{G12D}$ or pancreatic injury. Furthermore, a role for *Sox9* in conferring certain ductal characteristics to cells has recently been demonstrated in a model of surgically-induced pancreatitis (Prevot et al., 2012). While *Sox9* promotes ADM and ADR in gain-of-function experiments, our results show that tissue injury can still, to some extent, induce ADM from *Sox9*-deficient acinar cells. This suggests that other factors can compensate for Sox9 during injury-induced ADM. One candidate is the duct-specific transcription factor Hnf6, which is induced in acinar cells by pancreatic injury and is both necessary and sufficient for ADM (Prevot et al., 2012). In the absence of *Sox9*, however, Hnf6 is less efficient in inducing CK19 (Prevot et al., 2012), suggesting synergy between Hnf6 and Sox9 during ductal conversion of acinar cells. Different from Sox9, Hnf6 expression is not maintained in PanINs and PDA (Prevot et al., 2012). Therefore, only Sox9 expression is sustained in PanINs, providing a possible explanation for why Sox9 is absolutely required for PanIN formation.

Acinar-derived duct-like lesions and pancreatic ducts display similar molecular and morphological features, yet PanINs emerge more readily from acinar-derived duct-like cells than ductal cells. This implies that duct-like lesions differ from native pancreatic ducts. The transcription factors Sox9, Hnf6 and Hes1 are not only markers for pancreatic ductal cells, but are also expressed in multipotent progenitors of the developing pancreas (Jacquemin et al., 2003; Miyamoto et al., 2003; Seymour et al., 2007), raising the question of whether ADM is truly ductal in nature or more closely resembles embryonic progenitors. Previous studies have suggested that ADM lesions are similar to immature embryonic progenitor-like cells because they express Pdx1, Nestin, and Hes1 (Jensen et al., 2005; Miyamoto et al., 2003; Shi et al., 2012; Song et al., 1999). However, multipotent progenitor markers, such as Hnf1b and Nkx6.1 (Schaffer et al., 2010; Solar et al., 2009), are not present in acinar-derived duct-like cells (Jensen et al., 2005; Prevot et al., 2012) indicating that these cells may resemble an acinar-committed yet still immature Nestin-positive progenitor cell (Carriere et al., 2007; Esni et al., 2004). Comparative transcriptome analysis of these different native and transformed cell populations will shed light on the molecular differences between these populations and could provide clues as to why PanINs readily emerge from acinar cells, but not ducts, in response to oncogenic Kras.

The role of acinar-to-ductal metaplasia in the initiation of pancreatic neoplasia

Our finding that PanINs predominantly originate from acinar cells identifies the transition of acinar cells into a duct-like state as an important early event in tumor initiation. In addition to induction of ductal genes, destabilization of the acinar cell phenotype appears to also

promote ADM and PanINs, as evidenced by an acceleration in *Kras*^{G12D}-mediated ADM and PanIN formation after deletion of the acinar-restricted transcription factor *Mist1* (Shi et al., 2009; Shi et al., 2012). This suggests that the observed synergy between oncogenic Kras and *Sox9* misexpression or pancreatic injury in PanIN initiation might be a result of each condition increasing acinar cell plasticity. Therefore, known risk factors for PDA, such as chronic pancreatitis or genetic variants of acinar-specific genes (Li et al., 2012; Lowenfels et al., 1993; Lowenfels et al., 1997), may increase PDA risk by rendering acinar cells more plastic and reducing the threshold for ADM. It is important to note that a direct lineage relationship between ADM and PanINs has yet to be formally demonstrated and the possibility remains that ADM lesions do not directly transition into PanINs. However, it is clear that both ADM and PanIN lesions arise from acinar cells (Guerra et al., 2007; Morris et al., 2010) and that reducing ADM formation through inhibition of the EGFR pathway or overexpression of pro-acinar genes reduces Kras^{G12D}-induced PanINs (Ardito et al., 2012; Navas et al., 2012; Shi et al., 2012). This suggests that pathways critical for ADM are also necessary for PanIN formation.

Our results imply that therapeutic targeting of signaling pathways involved in ductal reprogramming of acinar cells could prevent PDA initiation. Previous studies have demonstrated that the EGFR, Hedgehog and Notch signaling pathways promote ADM and PanIN formation (De La O et al., 2008; Fendrich et al., 2008; Miyamoto et al., 2003; Pasca di Magliano et al., 2006; Rajurkar et al., 2012; Siveke et al., 2007). Interestingly, these pathways are known to be up-stream regulators of Sox9 expression in multiple organs (Bien-Willner et al., 2007; Haller et al., 2012; Ling et al., 2010; Meier-Stiegen et al., 2010; Muto et al., 2009; Zong et al., 2009). Moreover, Notch signaling has recently been shown to control *Sox9* expression and induce ductal genes in the pancreas (Delous et al., 2012; Manfroid et al., 2012; Shih et al., 2012). Therefore, it is possible that Sox9 is the critical effector of Notch during PanIN induction. Consistent with this notion, inhibition of Notch signaling in the presence of oncogenic Kras reduced PanIN formation (Plentz et al., 2009), similar to *Sox9* inactivation in our current study. However, it remains to be examined how inputs from different signaling pathways converge on Sox9 to promote PanIN initiation. Our findings now pave the way for future studies exploring whether the inhibition of acinar cell plasticity could have therapeutic applications in the prophylaxis of PDA in high-risk individuals.

Experimental Procedures

Mouse Procedures

All animal experiments described herein were approved by the University of California, San Diego and San Francisco Institutional Animal Care and Use Committees. The sources for mouse strains as well as genotyping and glucose measurement strategies are described in the Supplemental Experimental Procedures. Tamoxifen (Sigma-Aldrich) was dissolved in corn oil and administered subcutaneously at 5 mg/40 g per injection. Mice were injected with caerulein (50 μg/kg diluted in saline; Sigma-Aldrich) or saline on two alternating days once every hour for six hours each day (used in experiments with *Kras*^{G12D} mice) or on two consecutive days once every hour for eight hours each day (used in experiments in absence of *Kras*^{G12D} allele) (Morris et al., 2010).

Histology, Immunohistochemical and Immunofluorescence Analysis

Paraffin-embedded or frozen sections were subjected to hematoxylin (Mayers or Harris formulations), eosin, Alcian blue, nuclear fast red (Vector Labs), immunohistochemical or immunofluorescence staining as described (Morris et al., 2010; Seymour et al., 2007; Seymour et al., 2008). Detailed procedures for histological and morphometric analyses, as

well as a list of primary and secondary antibodies can be found in the Supplemental Experimental Procedures.

Statistical Analysis

P-values were calculated using the two-tailed student's t-test with the GraphPad Prism or Excel software.

Supplementary Material

Refer to Web version on PubMed Central for supplementary material.

Acknowledgments

We thank Nissi Varki (UCSD Cancer Center, Histopathology Core), Cecilia Austin, Jimmy Chen, Nancy Rosenblatt, Sangho Yu, and Kai En Tang for expert technical assistance and Andrew Lowy and members of the Sander and Hebrok laboratories for discussions and comments on the manuscript. For mouse lines and antibodies, we would like to thank: David Tuveson, (UK Cambridge Research Institute; $Kras^{G12D}$ mice), Gerd Scherer (University of Freiburg; $Sox9^{flox}$ mice), and Chrissa Kioussi (Oregon State University; anti-GFP antibody). Microscopy was supported by resources from the UCSF Diabetes and Endocrinology Research Center (DERC). This work was supported by NIH-R01DK078803 to M.S., NIH-R01CA112537 to M.H., NIH-F32CA136124 to J.L.K. and DFG-FI1719/1-1 to G.V.F.

References

Aguirre AJ, Bardeesy N, Sinha M, Lopez L, Tuveson DA, Horner J, Redston MS, DePinho RA. Activated Kras and Ink4a/Arf deficiency cooperate to produce metastatic pancreatic ductal adenocarcinoma. Genes Dev. 2003; 17:3112–3126. [PubMed: 14681207]

Ardito CM, Gruner BM, Takeuchi KK, Lubeseder-Martellato C, Teichmann N, Mazur PK, Delgiorno KE, Carpenter ES, Halbrook CJ, Hall JC, et al. EGF Receptor Is Required for KRAS-Induced Pancreatic Tumorigenesis. Cancer Cell. 2012; 22:304–317. [PubMed: 22975374]

Bien-Willner GA, Stankiewicz P, Lupski JR. SOX9cre1, a cis-acting regulatory element located 1.1 Mb upstream of SOX9, mediates its enhancement through the SHH pathway. Hum Mol Genet. 2007; 16:1143–1156. [PubMed: 17409199]

Brembeck FH, Schreiber FS, Deramaudt TB, Craig L, Rhoades B, Swain G, Grippo P, Stoffers DA, Silberg DG, Rustgi AK. The mutant K-ras oncogene causes pancreatic periductal lymphocytic infiltration and gastric mucous neck cell hyperplasia in transgenic mice. Cancer Res. 2003; 63:2005–2009. [PubMed: 12727809]

Carriere C, Seeley ES, Goetze T, Longnecker DS, Korc M. The Nestin progenitor lineage is the compartment of origin for pancreatic intraepithelial neoplasia. Proc Natl Acad Sci U S A. 2007; 104:4437–4442. [PubMed: 17360542]

Carriere C, Young AL, Gunn JR, Longnecker DS, Korc M. Acute pancreatitis markedly accelerates pancreatic cancer progression in mice expressing oncogenic Kras. Biochem Biophys Res Commun. 2009; 382:561–565. [PubMed: 19292977]

Cornish TC, Hruban RH. Pancreatic Intraepithelial Neoplasia. Surgical Pathology Clinics. 2011; 4:523–535.

De La O JP, Emerson LL, Goodman JL, Froebe SC, Illum BE, Curtis AB, Murtaugh LC. Notch and Kras reprogram pancreatic acinar cells to ductal intraepithelial neoplasia. Proc Natl Acad Sci U S A. 2008; 105:18907–18912. [PubMed: 19028876]

De La O JP, Murtaugh LC. Notch and Kras in pancreatic cancer: at the crossroads of mutation, differentiation and signaling. Cell cycle. 2009; 8:1860–1864. [PubMed: 19440048]

Delous M, Yin C, Shin D, Ninov N, Debrito Carten J, Pan L, Ma TP, Farber SA, Moens CB, Stainier DYR. sox9b Is a Key Regulator of Pancreaticobiliary Ductal System Development. PLoS genetics. 2012; 8:e1002754. [PubMed: 22719264]

Desai BM, Oliver-Krasinski J, De Leon DD, Farzad C, Hong N, Leach SD, Stoffers DA. Preexisting pancreatic acinar cells contribute to acinar cell, but not islet beta cell, regeneration. J Clin Invest. 2007; 117:971–977. [PubMed: 17404620]

Esni F, Stoffers DA, Takeuchi T, Leach SD. Origin of exocrine pancreatic cells from nestin-positive precursors in developing mouse pancreas. Mech Dev. 2004; 121:15–25. [PubMed: 14706696]

Feldmann G, Beaty R, Hruban RH, Maitra A. Molecular genetics of pancreatic intraepithelial neoplasia. J Hepatobiliary Pancreat Surg. 2007; 14:224–232. [PubMed: 17520196]

Fendrich V, Esni F, Garay MV, Feldmann G, Habbe N, Jensen JN, Dor Y, Stoffers D, Jensen J, Leach SD, Maitra A. Hedgehog signaling is required for effective regeneration of exocrine pancreas. Gastroenterology. 2008; 135:621–631. [PubMed: 18515092]

Gidekel Friedlander SY, Chu GC, Snyder EL, Girnius N, Dibelius G, Crowley D, Vasile E, DePinho RA, Jacks T. Context-dependent transformation of adult pancreatic cells by oncogenic K-Ras. Cancer Cell. 2009; 16:379–389. [PubMed: 19878870]

Goldstein AS, Huang J, Guo C, Garraway IP, Witte ON. Identification of a cell of origin for human prostate cancer. Science. 2010; 329:568–571. [PubMed: 20671189]

Guerra C, Schuhmacher AJ, Canamero M, Grippo PJ, Verdaguer L, Perez-Gallego L, Dubus P, Sandgren EP, Barbacid M. Chronic pancreatitis is essential for induction of pancreatic ductal adenocarcinoma by K-Ras oncogenes in adult mice. Cancer Cell. 2007; 11:291–302. [PubMed: 17349585]

Habbe N, Shi G, Meguid RA, Fendrich V, Esni F, Chen H, Feldmann G, Stoffers DA, Konieczny SF, Leach SD, Maitra A. Spontaneous induction of murine pancreatic intraepithelial neoplasia (mPanIN) by acinar cell targeting of oncogenic Kras in adult mice. Proc Natl Acad Sci U S A. 2008; 105:18913–18918. [PubMed: 19028870]

Haller R, Schwanbeck R, Martini S, Bernoth K, Kramer J, Just U, Rohwedel J. Notch1 signaling regulates chondrogenic lineage determination through Sox9 activation. Cell Death Differ. 2012; 19:461–469. [PubMed: 21869831]

Heiser PW, Cano DA, Landsman L, Kim GE, Kench JG, Klimstra DS, Taketo MM, Biankin AV, Hebrok M. Stabilization of beta-catenin induces pancreas tumor formation. Gastroenterology. 2008; 135:1288–1300. [PubMed: 18725219]

Hezel AF, Kimmelman AC, Stanger BZ, Bardeesy N, Depinho RA. Genetics and biology of pancreatic ductal adenocarcinoma. Genes Dev. 2006; 20:1218–1249. [PubMed: 16702400]

Hingorani SR, Petricoin EF, Maitra A, Rajapakse V, King C, Jacobetz MA, Ross S, Conrads TP, Veenstra TD, Hitt BA, et al. Preinvasive and invasive ductal pancreatic cancer and its early detection in the mouse. Cancer Cell. 2003; 4:437–450. [PubMed: 14706336]

Hingorani SR, Wang L, Multani AS, Combs C, Deramaudt TB, Hruban RH, Rustgi AK, Chang S, Tuveson DA. Trp53R172H and KrasG12D cooperate to promote chromosomal instability and widely metastatic pancreatic ductal adenocarcinoma in mice. Cancer Cell. 2005; 7:469–483. [PubMed: 15894267]

Jacquemin P, Lemaigre FP, Rousseau GG. The Onecut transcription factor HNF-6 (OC-1) is required for timely specification of the pancreas and acts upstream of Pdx-1 in the specification cascade. Developmental Biology. 2003; 258:105–116. [PubMed: 12781686]

Jensen JN, Cameron E, Garay MV, Starkey TW, Gianani R, Jensen J. Recapitulation of elements of embryonic development in adult mouse pancreatic regeneration. Gastroenterology. 2005; 128:728–741. [PubMed: 15765408]

Kanda M, Matthaei H, Wu J, Hong SM, Yu J, Borges M, Hruban RH, Maitra A, Kinzler K, Vogelstein B, Goggins M. Presence of somatic mutations in most early-stage pancreatic intraepithelial neoplasia. Gastroenterology. 2012; 142:730–733. e739. [PubMed: 22226782]

Kopp JL, Dubois CL, Schaffer AE, Hao E, Shih HP, Seymour PA, Ma J, Sander M. Sox9+ ductal cells are multipotent progenitors throughout development but do not produce new endocrine cells in the normal or injured adult pancreas. Development. 2011; 138:653–665. [PubMed: 21266405]

Li D, Duell EJ, Yu K, Risch HA, Olson SH, Kooperberg C, Wolpin BM, Jiao L, Dong X, Wheeler B, et al. Pathway Analysis of Genome-wide Association Study Data Highlights Pancreatic Development Genes as Susceptibility Factors for Pancreatic Cancer. Carcinogenesis. 2012

Ling H, Sylvestre JR, Jolicoeur P. Notch1-induced mammary tumor development is cyclin D1-dependent and correlates with expansion of pre-malignant multipotent duct-limited progenitors. Oncogene. 2010; 29:4543–4554. [PubMed: 20562911]

Lowenfels AB, Maisonneuve P, Cavallini G, Ammann RW, Lankisch PG, Andersen JR, Dimagno EP, Andren-Sandberg A, Domellof L. Pancreatitis and the risk of pancreatic cancer. International Pancreatitis Study Group. N Engl J Med. 1993; 328:1433–1437. [PubMed: 8479461]

Lowenfels AB, Maisonneuve P, DiMagno EP, Elitsur Y, Gates LK Jr, Perrault J, Whitcomb DC. Hereditary pancreatitis and the risk of pancreatic cancer. International Hereditary Pancreatitis Study Group. J Natl Cancer Inst. 1997; 89:442–446. [PubMed: 9091646]

Manfroid I, Ghaye A, Naye F, Detry N, Palm S, Pan L, Ma TP, Huang W, Rovira M, Martial JA, et al. Zebrafish sox9b is crucial for hepatopancreatic duct development and pancreatic endocrine cell regeneration. Dev Biol. 2012; 366:268–278. [PubMed: 22537488]

Meier-Stiegen F, Schwanbeck R, Bernoth K, Martini S, Hieronymus T, Ruau D, Zenke M, Just U. Activated Notch1 target genes during embryonic cell differentiation depend on the cellular context and include lineage determinants and inhibitors. PLoS ONE. 2010; 5:e11481. [PubMed: 20628604]

Miyamoto Y, Maitra A, Ghosh B, Zechner U, Argani P, Iacobuzio-Donahue CA, Sriuranpong V, Iso T, Meszoely IM, Wolfe MS, et al. Notch mediates TGF alpha-induced changes in epithelial differentiation during pancreatic tumorigenesis. Cancer Cell. 2003; 3:565–576. [PubMed: 12842085]

Morris JP, Cano DA, Sekine S, Wang SC, Hebrok M. Beta-catenin blocks Kras-dependent reprogramming of acini into pancreatic cancer precursor lesions in mice. J Clin Invest. 2010; 120:508–520. [PubMed: 20071774]

Muto A, Iida A, Satoh S, Watanabe S. The group E Sox genes Sox8 and Sox9 are regulated by Notch signaling and are required for Muller glial cell development in mouse retina. Exp Eye Res. 2009; 89:549–558. [PubMed: 19490914]

Navas C, Hernandez-Porras I, Schuhmacher AJ, Sibilia M, Guerra C, Barbacid M. EGF receptor signaling is essential for k-ras oncogene-driven pancreatic ductal adenocarcinoma. Cancer Cell. 2012; 22:318–330. [PubMed: 22975375]

Pasca di Magliano M, Sekine S, Ermilov A, Ferris J, Dlugosz AA, Hebrok M. Hedgehog/Ras interactions regulate early stages of pancreatic cancer. Genes Dev. 2006; 20:3161–3173. [PubMed: 17114586]

Plentz R, Park JS, Rhim AD, Abravanel D, Hezel AF, Sharma SV, Gurumurthy S, Deshpande V, Kenific C, Settleman J, et al. Inhibition of gamma-secretase activity inhibits tumor progression in a mouse model of pancreatic ductal adenocarcinoma. Gastroenterology. 2009; 136:1741–1749. e1746. [PubMed: 19208345]

Prevot PP, Simion A, Grimont A, Colletti M, Khalaileh A, Van den Steen G, Sempoux C, Xu X, Roelants V, Hald J, et al. Role of the ductal transcription factors HNF6 and Sox9 in pancreatic acinar-to-ductal metaplasia. Gut. 2012 On-line First: 22 January 2012.

Rajurkar M, De Jesus-Monge WE, Driscoll DR, Appleman VA, Huang H, Cotton JL, Klimstra DS, Zhu LJ, Simin K, Xu L, et al. The activity of Gli transcription factors is essential for Kras-induced pancreatic tumorigenesis. Proc Natl Acad Sci U S A. 2012; 109:E1038–1047. [PubMed: 22493246]

Ray KC, Bell KM, Yan J, Gu G, Chung CH, Washington MK, Means AL. Epithelial Tissues Have Varying Degrees of Susceptibility to KrasG12D-Initiated Tumorigenesis in a Mouse Model. PLoS ONE. 2011; 6:e16786. [PubMed: 21311774]

Rovira M, Scott SG, Liss AS, Jensen J, Thayer SP, Leach SD. Isolation and characterization of centroacinar/terminal ductal progenitor cells in adult mouse pancreas. Proc Natl Acad Sci U S A. 2010; 107:75–80. [PubMed: 20018761]

Schaffer AE, Freude KK, Nelson SB, Sander M. Nkx6 transcription factors and Ptf1a function as antagonistic lineage determinants in multipotent pancreatic progenitors. Dev Cell. 2010; 18:1022–1029. [PubMed: 20627083]

Seymour PA, Freude KK, Tran MN, Mayes EE, Jensen J, Kist R, Scherer G, Sander M. SOX9 is required for maintenance of the pancreatic progenitor cell pool. Proc Natl Acad Sci U S A. 2007; 104:1865–1870. [PubMed: 17267606]

Seymour PA, Freude KK, Dubois CL, Shih HP, Patel NA, Sander M. A dosage-dependent requirement for Sox9 in pancreatic endocrine cell formation. Dev Biol. 2008; 323:19–30. [PubMed: 18723011]

Shi G, Zhu L, Sun Y, Bettencourt R, Damsz B, Hruban RH, Konieczny SF. Loss of the acinar-restricted transcription factor Mist1 accelerates Kras-induced pancreatic intraepithelial neoplasia. Gastroenterology. 2009; 136:1368–1378. [PubMed: 19249398]

Shi G, Direnzo D, Qu C, Barney D, Miley D, Konieczny SF. Maintenance of acinar cell organization is critical to preventing Kras-induced acinar-ductal metaplasia. Oncogene. 2012 Jun 4. [E-pub ahead of print].

Shih HP, Kopp JL, Sandhu M, Dubois CL, Seymour PA, Grapin-Botton A, Sander M. A Notch-dependent molecular circuitry initiates pancreatic endocrine and ductal cell differentiation. Development. 2012; 139:2488–2499. [PubMed: 22675211]

Siveke JT, Einwachter H, Sipos B, Lubeseder-Martellato C, Kloppel G, Schmid RM. Concomitant pancreatic activation of Kras(G12D) and Tgfa results in cystic papillary neoplasms reminiscent of human IPMN. Cancer Cell. 2007; 12:266–279. [PubMed: 17785207]

Solar M, Cardalda C, Houbracken I, Martin M, Maestro MA, De Medts N, Xu X, Grau V, Heimberg H, Bouwens L, Ferrer J. Pancreatic exocrine duct cells give rise to insulin-producing beta cells during embryogenesis but not after birth. Dev Cell. 2009; 17:849–860. [PubMed: 20059954]

Song SY, Gannon M, Washington MK, Scoggins CR, Meszoely IM, Goldenring JR, Marino CR, Sandgren EP, Coffey RJ Jr, Wright CV, Leach SD. Expansion of Pdx1-expressing pancreatic epithelium and islet neogenesis in transgenic mice overexpressing transforming growth factor alpha. Gastroenterology. 1999; 117:1416–1426. [PubMed: 10579983]

Stanger BZ, Stiles B, Lauwers GY, Bardeesy N, Mendoza M, Wang Y, Greenwood A, Cheng KH, McLaughlin M, Brown D, et al. Pten constrains centroacinar cell expansion and malignant transformation in the pancreas. Cancer Cell. 2005; 8:185–195. [PubMed: 16169464]

Strobel O, Dor Y, Alsina J, Stirman A, Lauwers G, Trainor A, Castillo CF, Warshaw AL, Thayer SP. In vivo lineage tracing defines the role of acinar-to-ductal transdifferentiation in inflammatory ductal metaplasia. Gastroenterology. 2007; 133:1999–2009. [PubMed: 18054571]

Strobel O, Rosow DE, Rakhlin EY, Lauwers GY, Trainor AG, Alsina J, Fernandez-Del Castillo C, Warshaw AL, Thayer SP. Pancreatic duct glands are distinct ductal compartments that react to chronic injury and mediate Shh-induced metaplasia. Gastroenterology. 2010; 138:1166–1177. [PubMed: 20026066]

Visvader JE. Cells of origin in cancer. Nature. 2011; 469:314–322. [PubMed: 21248838]

Ying H, Elpek KG, Vinjamoori A, Zimmerman SM, Chu GC, Yan H, Fletcher-Sananikone E, Zhang H, Liu Y, Wang W, et al. PTEN is a major tumor suppressor in pancreatic ductal adenocarcinoma and regulates an NF-kappaB-cytokine network. Cancer Discov. 2011; 1:158–169. [PubMed: 21984975]

Zhu L, Shi G, Schmidt CM, Hruban RH, Konieczny SF. Acinar cells contribute to the molecular heterogeneity of pancreatic intraepithelial neoplasia. Am J Pathol. 2007; 171:263–273. [PubMed: 17591971]

Zong Y, Panikkar A, Xu J, Antoniou A, Raynaud P, Lemaigre F, Stanger BZ. Notch signaling controls liver development by regulating biliary differentiation. Development. 2009; 136:1727–1739. [PubMed: 19369401]

Significance

PDA has a dismal prognosis, largely because it is mostly diagnosed at an advanced stage. For developing early detection methods and treatments, it is essential to understand the primary events leading to tumor initiation. By tracing specific cell populations in the presence and absence of tissue injury in mice, we demonstrate that oncogenic Kras can readily induce PDA precursor lesions from adult pancreatic acinar cells, but not from ductal or centroacinar cells. Moreover, using loss- and gain-of-function approaches we identify the ductal fate determinant *Sox9* as a critical mediator of Kras-induced premalignant acinar cell reprogramming. Our findings demonstrate a key role for acinar cells in PDA initiation and reveal Sox9 as a potential target for preventing early tumor-initiating events.

Highlights

1. Preneoplastic lesions rarely arise from pancreatic ductal/centroacinar cells
2. Acinar cells are the predominant cells of origin for pancreatic preneoplastic lesions
3. Initiation of pancreatic cancer depends on acinar induction of the ductal gene Sox9
4. Sox9 synergizes with $Kras^{G12D}$ and injury in acinar-to-ductal cell reprogramming

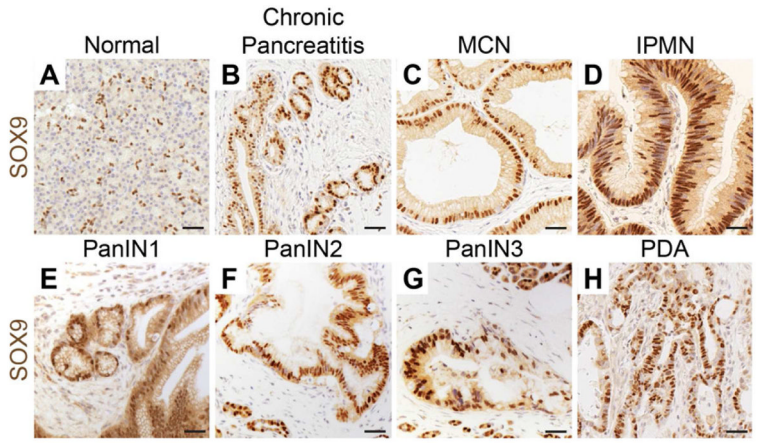

I

Category	Intensity of SOX9 expression		
	Negative	Weak	Strong
Normal	0/16 [0%]	16/16 [100%]	0/16 [0%]
Pancreatitis	2/16 [13%]	13/16 [81%]	1/16 [6%]
MCN	4/22 [18%]	13/22 [59%]	5/22 [23%]
IPMN	1/20 [5%]	13/20 [65%]	6/20 [30%]
PanIN 1-2	1/26 [4%]	12/26 [46%]	13/26 [50%]
PanIN 2-3	2/7 [29%]	2/7 [29%]	3/7 [43%]
PDA	6/19 [32%]	7/19 [37%]	6/19 [32%]

Figure 1. SOX9 is expressed in human premalignant and malignant pancreatic lesions

(**A**–**H**) Immunohistochemistry for SOX9 and hematoxylin counterstain on a tissue microarray spotted with human pancreatic tissue cores. Representative images showing SOX9 expression in normal pancreatic ducts (**A**), chronic pancreatitis (**B**), mucinous cystic neoplasms (MCN) (**C**), intraductal papillary mucinous neoplasms (IPMN) (**D**), pancreatic intraepithelial neoplasia 1 (PanIN1) (**E**), PanIN2 (**F**), PanIN3 (**G**), and pancreatic ductal adenocarcinoma (PDA) (**H**). (**I**) Number of tissue cores within each phenotypic category displaying no, weak, or strong SOX9 staining intensity. Scale bars: 100μm.

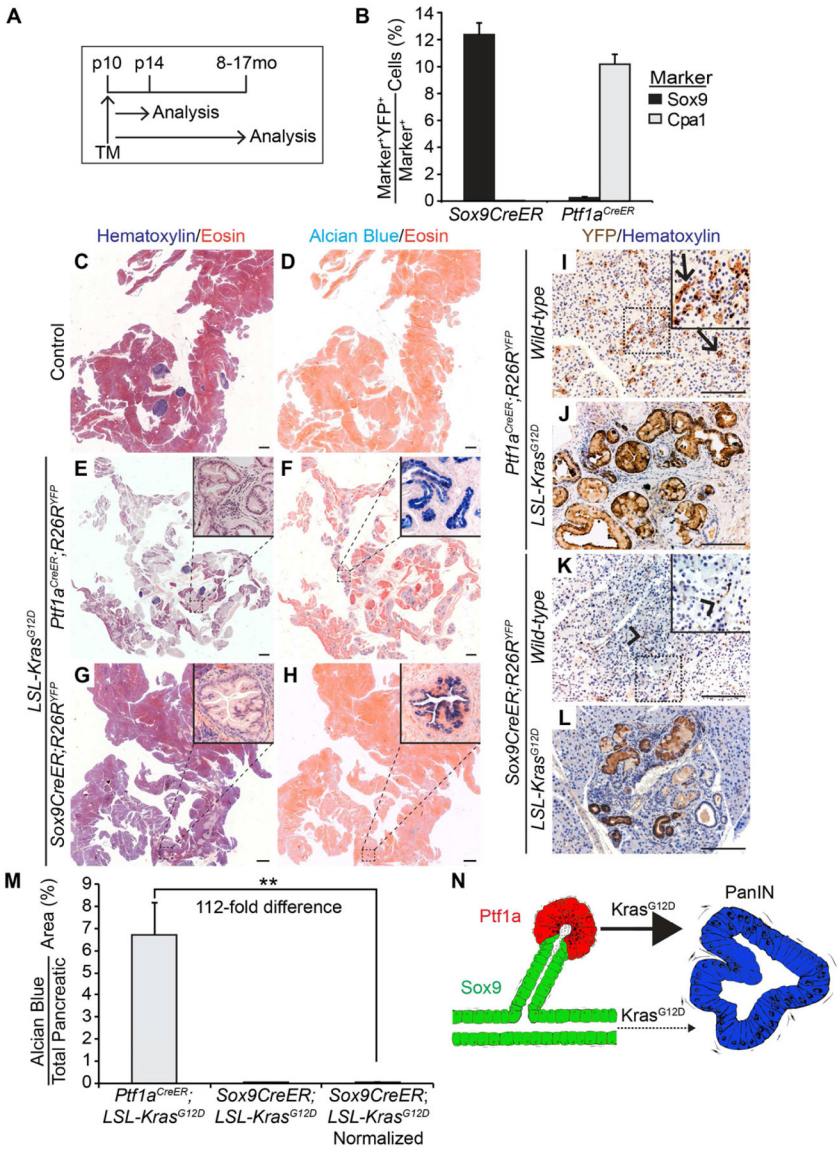

Figure 2. *Kras*^{G12D} expression in acinar, but not in ductal/centroacinar cells, readily induces PanIN formation

(**A**) *Sox9CreER;R26R*^{YFP} and *Ptf1a*^{CreER}*;R26R*^{YFP} mice were injected once with tamoxifen (TM) at postnatal day (p) 10 and analyzed at p14 or at 8 to 17 months (mo) of age. (**B**) Quantification of Sox9^{+} or Cpa1^{+} cells expressing YFP at p14 (n=4). H&E (**C, E, G**) or Alcian blue and eosin (**D, F, H**) staining of pancreatic sections from 8–17-month-old control (**C, D**), *Ptf1a*^{CreER}*;LSL-Kras*^{G12D}*;R26R*^{YFP} (**E, F**), or *Sox9CreER;LSL-Kras*^{G12D}*;R26R*^{YFP} (**G, H**) mice reveals abundant Alcian blue^{+} PanINs only in *Ptf1a*^{CreER}*;LSL-Kras*^{G12D}*;R26R*^{YFP} mice. (**I**–**L**) Immunohistochemistry of YFP in 8–17-month-old mice shows expression of YFP in acinar cells in *Ptf1a*^{CreER}*;R26R*^{YFP} mice (**I**, arrows) and ductal/centroacinar cells (CACs) in *Sox9CreER;R26R*^{YFP} mice (**K**, arrowheads). PanINs in *Ptf1a*^{CreER}*;LSL-Kras*^{G12D}*;R26R*^{YFP} (**J**) and *Sox9CreER;LSL-Kras*^{G12D}*;R26R*^{YFP} (**L**) mice are YFP^{+}, indicating an acinar or ductal/CAC origin, respectively. (**M**) Quantification of Alcian blue^{+} pancreatic area in 8–17-month-old mice (n=9 in *Ptf1a*^{CreER}*;LSL-Kras*^{G12D} mice; n=6 in *Sox9CreER;LSL-Kras*^{G12D} mice). The Alcian blue^{+} area in *Sox9CreER;LSL-*

Kras^{G12D};*R26R*^{YFP} mice was multiplied by 4.6 (normalized) to account for the greater total number of recombined cells in *Ptf1a*^{CreER};*R26R*^{YFP} mice (see Figure S1L). (**N**) Schematic showing the predominantly acinar origin of PanINs after expression of oncogenic Kras. Values are shown as mean ± s.e.m. ***P*<0.01. Scale bars: 1 mm (**C–H**) and 100μm (**I–L**). See also Figure S1.

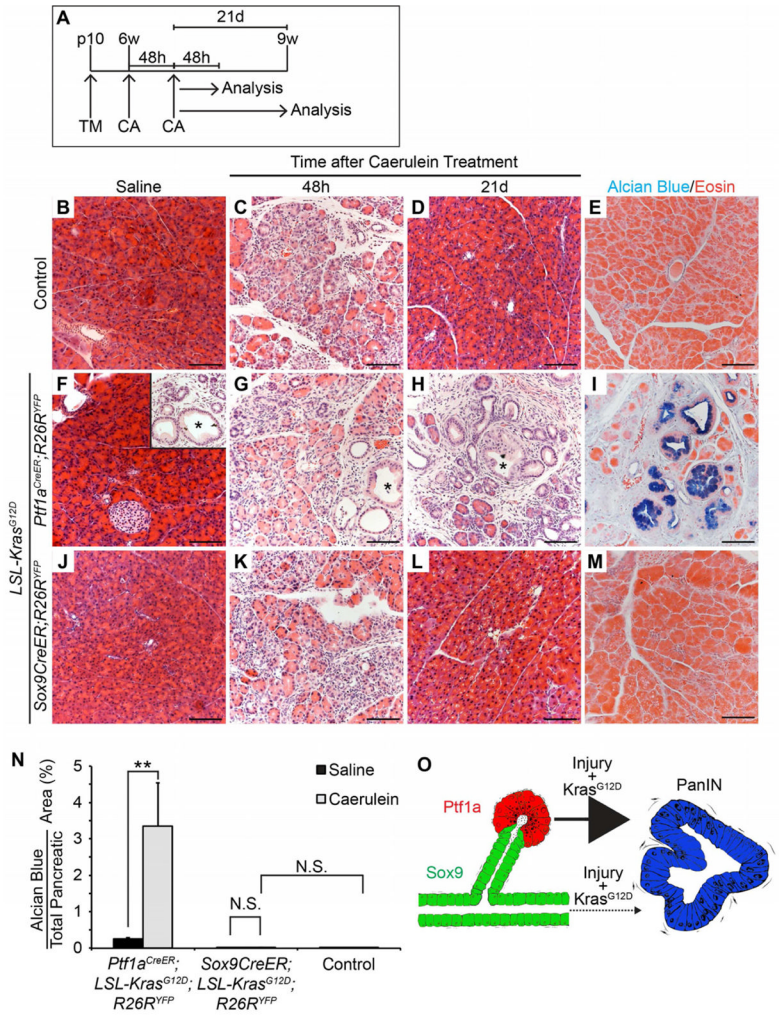

Figure 3. Acute pancreatitis promotes PanIN formation from *Kras*^{G12D}-expressing acinar cells, but not ductal/centroacinar cells

(**A**) *Ptf1a*^{CreER};*LSL-Kras*^{G12D};*R26R*^{YFP}, *Sox9CreER;LSL-Kras*^{G12D};*R26R*^{YFP} and control mice were injected once with tamoxifen (TM) at postnatal day (p) 10. At 6 weeks (w) of age, mice were treated with two sets of caerulein (CA) or saline injections on alternating days and analyzed 48 hours (h) or 21 days (d) later. (**B–D, F–H, J–L**) H&E staining reveals occasional PanINs in 9-week-old *Ptf1a*^{CreER};*LSL-Kras*^{G12D};*R26R*^{YFP} mice (**F**, inset) and persistent ADM and PanINs 21d after CA (**H**), but normal pancreas morphology in *Sox9CreER;LSL-Kras*^{G12D};*R26R*^{YFP} and control mice (**D, L**). Asterisks denote PanINs. (**E, I, M**) Alcian blue and eosin staining of pancreatic sections from mice 21d after CA treatment. (**N**) Quantification of Alcian blue^{+} pancreatic area reveals a significant increase in PanINs after CA in *Ptf1a*^{CreER};*LSL-Kras*^{G12D};*R26R*^{YFP} (n=4), but not in *Sox9CreER;LSL-Kras*^{G12D};*R26R*^{YFP} mice (n=5). (**O**) Schematic showing that pancreatic injury promotes PanIN formation from *Kras*^{G12D}-expressing acinar, but not ductal/centroacinar cells. N.S., not significant. Values are shown as mean ± s.e.m. ***P*<0.01. Scale bars: 100μm. See also Figure S2.

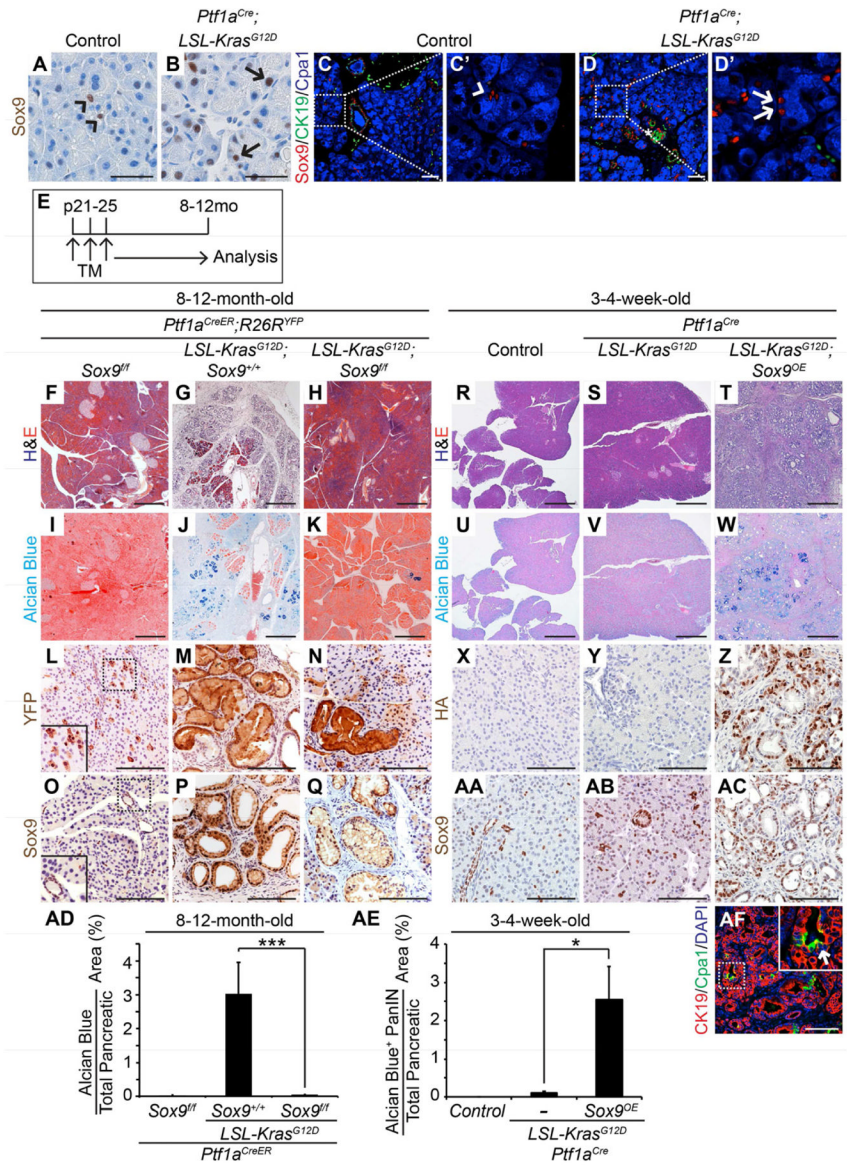

Figure 4. *Sox9* is necessary for and accelerates *Kras*^{G12D}-induced PanIN formation

(**A, B**) Immunohistochemistry shows Sox9 expression in ductal/centroacinar (CAC) (**A**, arrowheads), but not acinar cells in control mice. In 2-month-old *Ptf1a*^{Cre}*;LSL-Kras*^{G12D} mice, Sox9 is also detected in some acinar cells (**B**, arrows). (**C–D**) Co-immunofluorescence staining for Sox9, CK19 and Cpa1 confirms Sox9 expression in ductal/CACs (**C′**, arrowhead points to CAC) in control mice and shows Sox9^{+}Cpa1^{+}CK19^{-} acinar cells in *Ptf1a*^{Cre}*;LSL-Kras*^{G12D} mice (**D′**, arrowheads). (**E–Q**) Tamoxifen (TM) was administered to *Ptf1a*^{CreER}*;Sox9*$^{f/f}$*;R26R*^{YFP}, *Ptf1a*^{CreER}*;LSL-Kras*^{G12D}*;Sox9*$^{+/+}$*;R26R*^{YFP} and *Ptf1a*^{CreER}*;LSL-Kras*^{G12D}*;Sox9*$^{f/f}$*;R26R*^{YFP} mice at postnatal day (p) 21, 23 and 25 to simultaneously ablate *Sox9* and induce Kras^{G12D} in acinar cells. Mice were analyzed at 8–12 months (mo) of age. H&E (**F–H**) and Alcian blue staining (**I–K**) shows almost no PanINs after *Sox9* deletion. (**L–Q**) Immunohistochemistry reveals expression of YFP in PanINs in both *Ptf1a*^{CreER}*;Kras*^{G12D}*;Sox9*$^{+/+}$*;R26R*^{YFP} and *Ptf1a*^{CreER}*;LSL-Kras*^{G12D}*;Sox9*$^{f/f}$*;R26R*^{YFP} mice (**M, N**). Sox9 expression in PanINs in the *Sox9*$^{f/f}$ background indicates lack of *Sox9*^{f} recombination (**Q**). H&E (**R–T**) and Alcian blue

staining (**U–W**) reveals abundant ADM and PanINs in *Ptf1a*^{Cre};*LSL-Kras*^{G12D};*Sox9*^{OE}, but not in *Ptf1a*^{Cre};*LSL-Kras*^{G12D} or control mice at 3–4 weeks of age. Immunohistochemistry for HA (**X–Z**) and Sox9 (**AA–AC**) shows Sox9^{+} PanINs originating from cells that recombined the *Sox9*^{OE} transgene. (**AD, AE**) Quantification of Alcian blue^{+} pancreatic area reveals a significant reduction of PanINs after *Sox9* deletion (n=9) and conversely, an increase after *Sox9* misexpression (n=5). (**AF**) Immunofluorescence staining shows abundant CK19 and little Cpa1 expression in 4-week-old *Ptf1a*^{Cre};*LSL-Kras*^{G12D};*Sox9*^{OE} mice. Arrow points to CK19^{+}Cpa1^{+} cell. Values are shown as mean ± s.e.m. **P*<0.05 and ****P*<0.001. Scale bars: 25μm (**A–B**), 50 μm (**C, D**), 100 μm (**L–Q, X–AC, AF**), and 500μm (**F–K, R–W**). See also Figure S3.

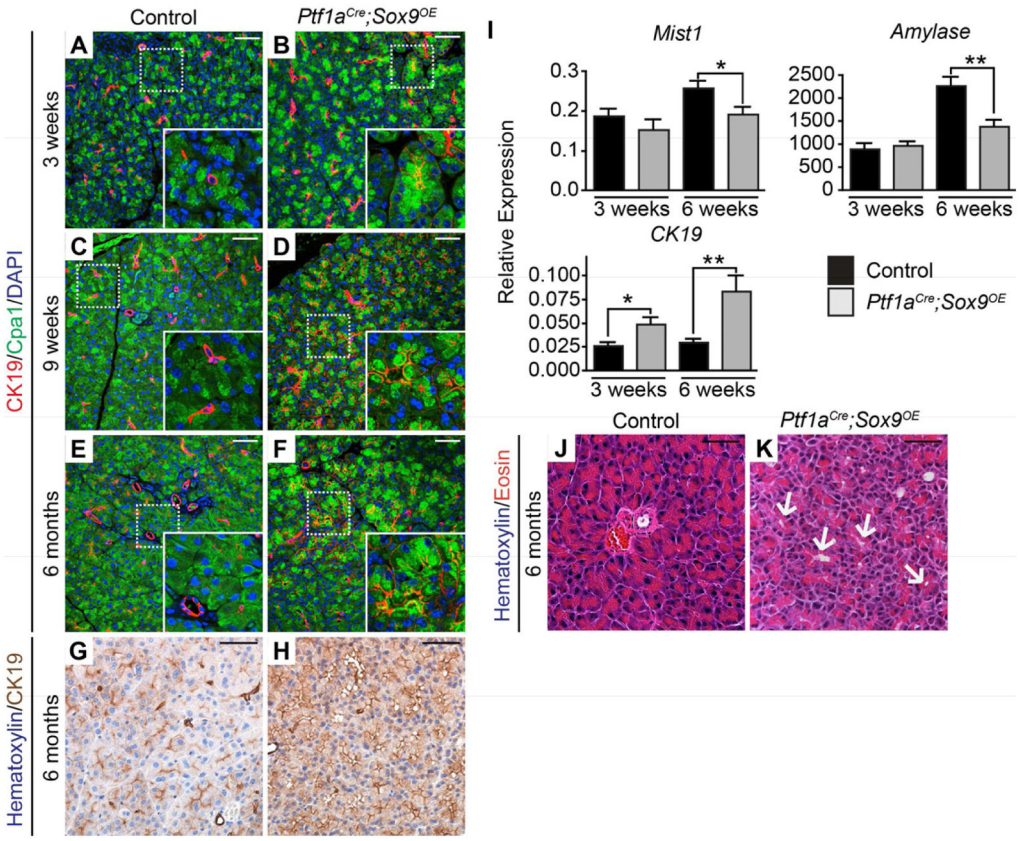

Figure 5. *Sox9* misexpression induces ductal genes

(**A–F**) Co-immunofluorescence staining for Cpa1 and CK19 shows $CK19^{+}Cpa^{+}$ cells in *Ptf1a*^{Cre};*Sox9*^{OE} mice (**B, D, F**), but not in controls (**A, C, E**). (**G–H**) Immunohistochemistry for CK19 reveals greater staining intensity in 6-month-old *Ptf1a*^{Cre};*Sox9*^{OE} than in control mice. (**I**) QRT-PCR analysis of *Mist1*, *amylase* and *CK19* in whole pancreas RNA from *Ptf1a*^{Cre};*Sox9*^{OE} and control mice (n=5). (**J, K**) H&E staining shows acinar clusters with dilated lumens in 6-month-old *Ptf1a*^{Cre};*Sox9*^{OE} mice (**K**, arrows). Values are shown as mean ± s.e.m. **P*<0.05 and ***P*<0.01. Scale bars: 50μm.

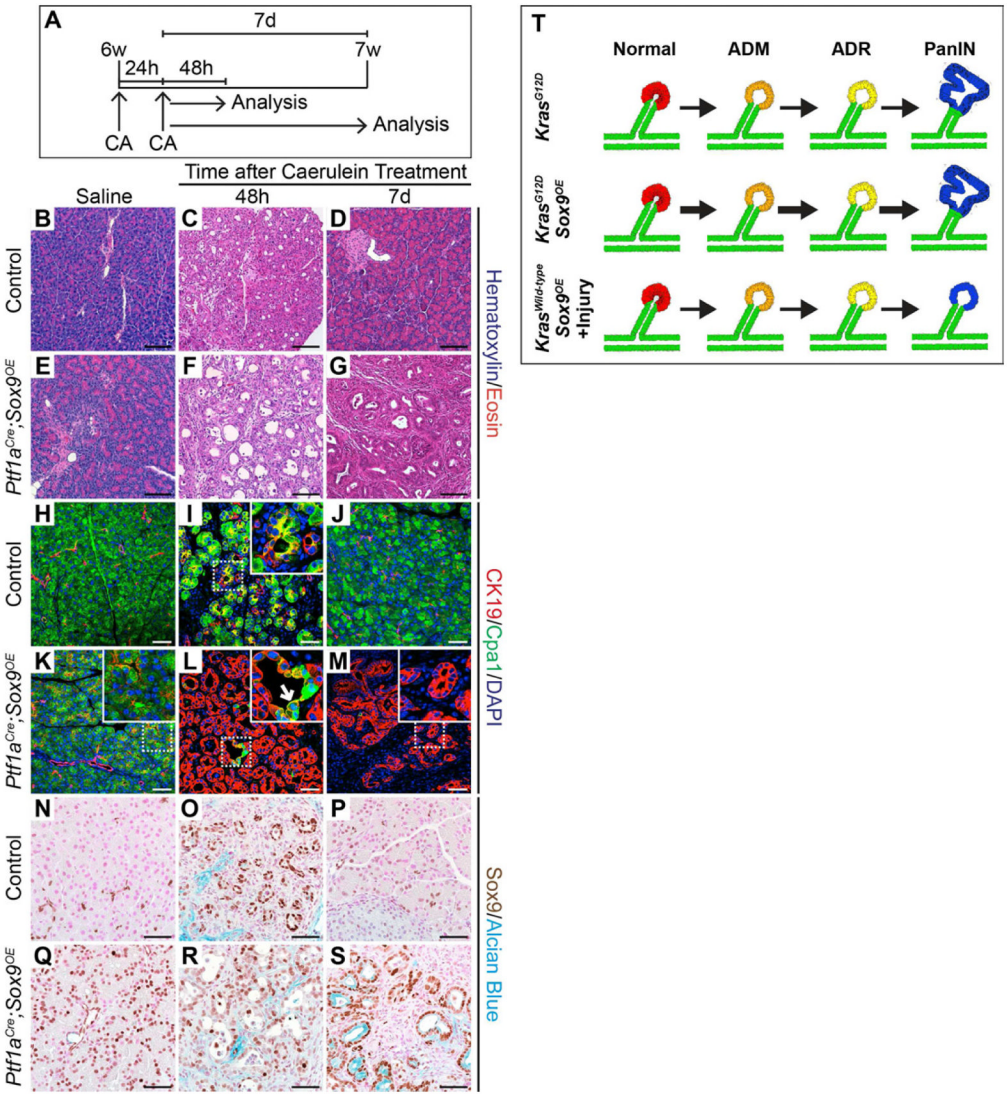

Figure 6. *Sox9* promotes persistent acinar-to-ductal reprogramming (ADR) and formation of mucinous metaplastic lesions after acute pancreatitis

(**A**) Six-week-old *Ptf1a*^{Cre};*Sox9*^{OE} and control mice were treated with two sets of caerulein (CA) or saline injections on consecutive days and analyzed 48 hours (h) or 7 days (d) later. Saline-treated mice were analyzed at 21d. (**B–G**) H&E staining reveals persistent acinar-to-ductal metaplasia (ADM) in *Ptf1a*^{Cre};*Sox9*^{OE} mice (**G**). (**H–M**) Co-immunofluorescence staining for CK19 and Cpa1 shows a few CK19^{+}Cpa1^{+} (**L,** arrow) 48h after CA and mainly CK19^{+}Cpa1^{-} cells after 7d (**M**) in *Ptf1a*^{Cre};*Sox9*^{OE} mice. (**N–S**) Immunohistochemistry for Sox9 and Alcian blue staining shows Sox9^{+}Alcian blue^{+} mucinous metaplastic lesions in *Ptf1a*^{Cre};*Sox9*^{OE} mice (**S**) but not in control mice (**P**) 7d after CA. (**T**) Schematic summarizing the phenotypes of *Sox9* misexpressing mice in the presence and absence of *Kras*^{G12D} or acute pancreatitis. w, weeks. Scale bars: 100μm (**B–G**) and 50μm (**H–S**). See also Figure S4.

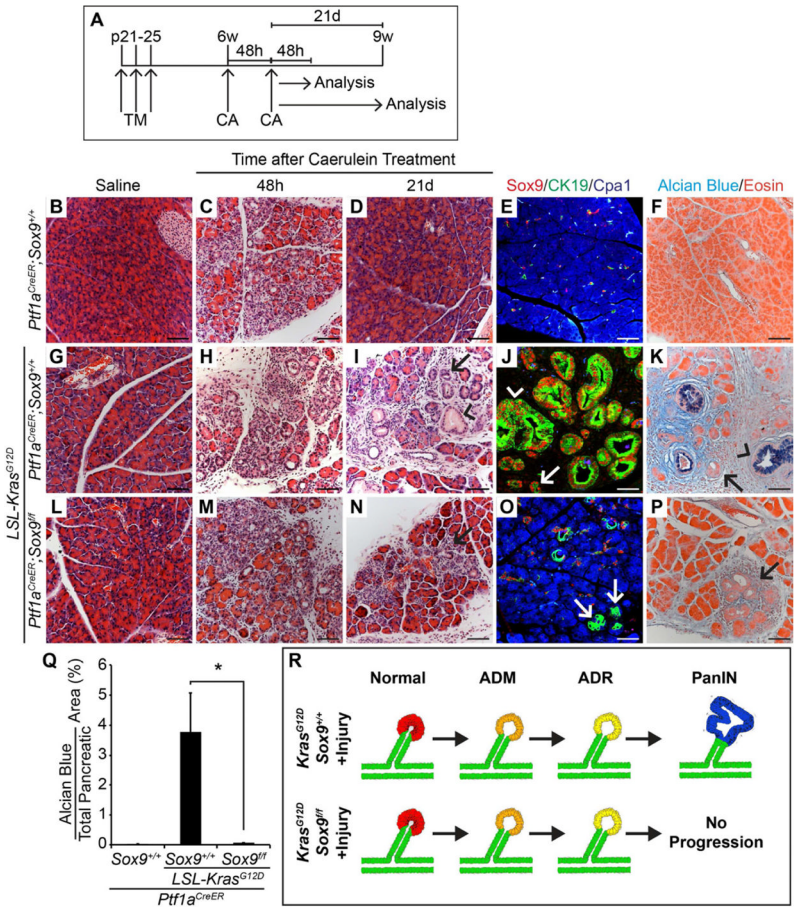

Figure 7. *Sox9*-deficient acinar cells expressing Kras^{G12D} can undergo persistent acinar-to-ductal reprogramming (ADR) after acute pancreatitis, but do not progress into PanINs

(**A**) *Ptf1a^{CreER};Sox9$^{+/+}$*, *Ptf1a^{CreER};LSL-Kras^{G12D};Sox9$^{+/+}$* and *Ptf1a^{CreER};LSL-Kras^{G12D};Sox9$^{f/f}$* mice were injected with tamoxifen (TM) at postnatal day (p) 21, 23 and 25. At 6 weeks (w) of age, mice were treated with two sets of caerulein (CA) or saline injections on alternating days and analyzed 48 hours (h) or 21 days (d) later. (**B–D, G–I, L–N**) H&E staining shows persistent acinar-to-ductal metaplasia (ADM) in *Ptf1a^{CreER};LSL-Kras^{G12D};Sox9$^{+/+}$* and to a lesser extent also in *Ptf1a^{CreER};LSL-Kras^{G12D};Sox9$^{f/f}$* mice (**I, N**, arrows). PanINs are only present in *Ptf1a^{CreER};LSL-Kras^{G12D};Sox9$^{+/+}$* mice (**I**, arrowhead). (**E, J, O**) Co-immunofluorescence staining for CK19, Cpa1 and Sox9 reveals CK19^{+}Cpa1^{-} duct-like cell clusters in *Ptf1a^{CreER};LSL-Kras^{G12D}* mice in the presence and absence of *Sox9* (**J, O**, arrows). (**F, K, P**) Alcian blue and eosin staining shows PanINs in *Ptf1a^{CreER};LSL-Kras^{G12D};Sox9$^{+/+}$* mice (**K**), but not in *Ptf1a^{CreER};LSL-Kras^{G12D};Sox9$^{f/f}$* mice (**P**). Arrows in **K, P** point to ADM and arrowheads in **J, K** to PanINs. (**Q**) Quantification of Alcian blue^{+} pancreatic area 21d after CA (n=4–5). (**R**) Schematic summarizing the phenotype observed in *Sox9* loss-of-function experiments in the presence of *Kras^{G12D}* and acute pancreatitis. Values are shown as mean ± s.e.m. *P<0.05. Scale bars: 50μm. See also Figure S5.

Table 1

Quantification of PanIN frequency in Ptf1a^{CreER};LSL-Kras^{G12D};R26R^{YFP} and Sox9CreER;LSL-Kras^{G12D};R26R^{YFP} mice

Genotype	N	Tamoxifen Injection Age (Days)	Analysis Age (Months)	Additional Treatment	Number of mice with PanINs (% of total mice)
Ptf1a^{CreER}; LSL-Kras^{G12D};R26R^{YFP}	12	10	8–17	None	12 (100%)
Sox9CreER; LSL- Kras^{G12D};R26R^{YFP}	14	10	8–16	None	8 (57%)
Ptf1a^{CreER}; LSL-Kras^{G12D};R26R^{YFP}	4	10	2	Caerulein	4 (100%)
Ptf1a^{CreER}; LSL-Kras^{G12D};R26R^{YFP}	4	10	2	Saline	4 (100%)
Sox9CreER; LSL-Kras^{G12D};R26R^{YFP}	5	10	2	Caerulein	3 (40%)
Sox9CreER; LSL-Kras^{G12D};R26R^{YFP}	9	10	2	Saline	1 (11%)

See also Table S1.